ONLINE FIRST

This is a provisional PDF only. Copyedited and fully formatted versión will be made available at final publication

HISTOLOGY AND HISTOPATHOLOGY

ISSN: 0213-3911
e-ISSN: 1699-5848

Submit your article to this Journal (http://www.hh.um.es/Instructions.htm)

Analysis of *wt1a* reporter line expression levels during proepicardium formation in the zebrafish

Authors: Laura Andrés-Delgado, María Galardi-Castilla, Nadia Mercader and Luis Santamaría

DOI: 10.14670/HH-18-238
Article type: JOURNAL ARTICLE
Accepted: 2020-07-07
Epub ahead of print: 2020-07-07

Analysis of *wt1a* reporter line expression levels during proepicardium formation in the zebrafish

Laura Andrés-Delgado[1,2,#], María Galardi-Castilla[2], Nadia Mercader[2,3] and Luis Santamaría[1]

1 Department of Anatomy, Histology and Neuroscience. School of Medicine. Autonoma University of Madrid. 28029 Madrid. Spain.

2. Development of the epicardium and its role during regeneration laboratory, Nacional Center of Cardiovascular Research Carlos III. 28029 Madrid, Spain.

3 Institute of Anatomy, University of Bern, 3000 Bern 9, Switzerland.

Corresponding author: Laura Andrés-Delgado, PhD. Departamento de Anatomía, Histología y Neurociencia, Facultad de Medicina, Universidad Autónoma de Madrid. C/ Arzobispo Morcillo, 4, 28029 Madrid, España. e-mail: laura.andresd@uam.es

Short running title: Wt1a levels in pericardial tissues

Key Words: Zebrafish, pericardial tissues, Cavalieri´s volume estimation, Bmp signaling

Summary: The epicardium is the outer mesothelial layer of the heart. It covers the myocardium and plays important roles in both heart development and regeneration. It is derived from the proepicardium (PE), groups of cells that emerges at early developmental stages from the dorsal pericardial layer (DP) close to the atrio-ventricular canal and the venous pole of the heart-tube. In zebrafish, PE cells extrude apically into the pericardial cavity as a consequence of DP tissue constriction, a process that is dependent on Bmp pathway signaling. Expression of the transcription factor *Wilms tumor-1*, *Wt1*, which is a leader of important morphogenetic events such as apoptosis regulation or epithelial-mesenchymal cell transition, is also necessary during PE formation. In this study, we used the zebrafish model to compare intensity level of the *wt1a* reporter line *epi:GFP* in PE and its original tissue, the DP. We found that GFP is present at higher intensity level in the PE tissue, and differentially *wt1* expression at pericardial tissues could be involved in the PE formation process. Our results reveal that *bmp2b* overexpression leads to enhanced GFP level both in DP and in PE tissues.

Introduction

The heart develops from the lateral plate mesoderm, and is one of the first organs to form and acquire its function. The primitive heart tube is composed of two layers, the myocardium and the endocardium, and during embryogenesis the third cellular layer of the heart, which is the epicardium, is developed. The epicardium covers the myocardium and influences it through paracrine signals that promote its growth and function (Olivey and Svensson, 2010; Perez-Pomares and de la Pompa, 2011). Also, epicardial-derived cells (EPDCs) can differentiate into other cell types as cardiac fibroblasts or adipocytes (Chau et al., 2014) and can contribute to the formation of the valves (Wessels et al., 2012; Duenas et al., 2017; Simoes and Riley, 2018). After heart injury, EPDCs can be involved in several aspects of tissue repair and regeneration (Kennedy-Lydon and Rosenthal, 2015).

The epicardium, also known as the visceral pericardium, has an extracardiac origin. It derives from the proepicardium (PE), transient groups of cells that emerge from the dorsal parietal pericardium (DP) in locations close to the atrio-ventricular canal (avc) and the venous pole (vp) of the heart tube. It appears around the time of heart looping and after the onset of heart beating (Schulte et al., 2007; Maya-Ramos et al., 2013; Kennedy-Lydon and Rosenthal, 2015). After PE is formed, the PE cells translocate and attach to the myocardial surface to form the epicardial layer (Manner et al., 2001).

How the PE is formed and how PE cells reach heart tube differs between models. In chicken, a temporary bridge forms between the PE and the myocardium and PE cells migrate

to the myocardial surface (Nahirney et al., 2003). Near aortic sac pericardium also contributes to epicardium formation in chicks (Perez-Pomares et al., 2003). In mice, a dual model was proposed. PE cells are transferred to the myocardium through direct contacts between the PE and the myocardium, and PE cells can be released into the pericardial cavity as floating clusters, which adhere to the myocardium (Rodgers et al., 2008; Li et al., 2017).

In zebrafish, three different PE populations were described (Peralta et al., 2013; Peralta et al., 2014): avcPE cluster; vpPE cluster; and arterial pole epicardial precursor cells (apPE), which are single pericardial cells at arterial pole site that directly contact the myocardium but barely contribute to epicardium. Once the avcPE and the vpPE cell clusters form, pericardial fluid flow generated by heartbeat stimulates PE cell aggregates to detach and reach the heart tube, spreading atop the myocardium to form a new tissue layer: the epicardium (Peralta et al., 2013). In combination with the floating PE clusters, a PE cellular bridge attached to the heart tube was also described in zebrafish (Plavicki et al., 2014). The differences obtained by the groups might be due to the different techniques and markers used. Plavicki et al. used fluorescent reporter driven by regulatory sequences of *tcf21*, a pan-epicardial marker, while the regulatory element of *wt1a* (*epi:GFP* reporter line*)*, which labels 70% of the PE cells, was used by Peralta and colleagues. Thereby, the combination of the results indicate that in zebrafish also a dual mechanism model for epicardial formation could be happening. PE formation in zebrafish is regulated by Bone morphogenetic protein (Bmp) pathway (Liu and Stainier, 2010), and Bmp signaling leads PE clusters formation by promoting actin cytoskeleton dynamics (Andres-Delgado et al., 2019).

There is a continuous rearrangement of tissue layers in the heart that affects cardiac morphogenesis (Andres-Delgado and Mercader, 2016; Collins and Stainier, 2016; Steed et al., 2016; Ocana et al., 2017). In zebrafish, the PE forms by a mechanism that involves the constriction of the DP layer and the apical extrusion of PE cell clusters to the pericardial cavity (Andres-Delgado et al., 2019). This suggests that an epithelial-mesenchymal-like transition (EMT) process could be taking place in the DP cells that transform into PE (Serluca, 2008; Wu et al., 2010; Tandon et al., 2016; Andres-Delgado et al., 2019). Wilms tumor 1 (WT1) has been implicated in regulating the EMT cell fate equilibrium in multiple contexts, including heart development (Smart et al., 2011) or cancer (Chau and Hastie, 2012). PE and epicardial layer presents expression of the transcription factor *wt1* in the larval zebrafish, and its presence is required for the determination of PE specification (Serluca, 2008). Wt1 expression in the PE has been postulated to be crucial for the development of this structure (Moore et al., 1999; Pombal et al., 2008; Serluca, 2008; Zeng et al., 2011). In mammals and avian epicardium, WT1 has been related with the maintenance of an intact epithelial morphology (Martinez-Estrada et al., 2010; Bax et al., 2011), and mutant analysis revealed an essential function of

WT1 during epicardial development as the null mice are not viable (Kreidberg et al., 1993; Moore et al., 1999; Carmona et al., 2001).

Here, we found that in the *wt1a* reporter line *epi:GFP,* GFP level is significantly higher in PE compared to the DP layer. Bmp signaling affects positively to the GFP intensity level in the different zebrafish pericardial tissues and favors the expression of *wt1a*.

Objectives

-To determine whether in zebrafish, tissue volume and GFP intensity level of the *wt1a* reporter line *epi:GFP* are similar in the dorsal pericardium compared to the proepicardium.

-To identify whether the overexpression of *bmp2b* regulates tissue volume and GFP intensity level of the *wt1a* reporter line *epi:GFP* in the dorsal pericardium and in the proepicardium of developing zebrafish.

-To determine whether *wt1a* expression level in dorsal pericardium and in the proepicardium is affected by Bmp2b.

Materials and methods

Zebrafish strains and husbandry

All experiments were approved by the Community of Madrid "Direccion General de Medio Ambiente", Spain. Animals were housed and experiments were performed in accordance with Spanish bioethical regulations for the use of laboratory animals. Zebrafish (*Danio rerio*) were maintained at a water temperature of 28 ºC. The following fish were used: wild-type AB strain (ZIRC, Eugene, OR, USA); *Et(-26.5Hsa.WT1-gata2:EGFP)*^{cn1} (hereafter termed *epi:GFP*) in which GFP expression is controlled by the regulatory elements of *wilms tumor 1a* (*wt1a*), and recapitulates its expression pattern (Peralta et al., 2013) and *Tg(hsp70l:bmp2b)*^{fr13} (Chocron et al., 2007).

Heat shock

In order to increase *bmp2b* levels at a specific developmental stage, the transgenic line *Tg(hsp70l:bmp2b)*^{fr13}, which overexpressed *bmp2b* under a heat-shock promoter, were heat shocked as follows: heat shocks were performed to the embryos at 39ºC in preheated water for 1 h at 26, 35 and 48 hpf (Andres-Delgado et al., 2019).

Animals treated with heat shocks were genotyped after confocal image acquisition. This

allowed unbiased comparison and blinded quantification of experimental and control groups.

Immunofluorescence

60 hpf embryos were fixed overnight in 4% paraformaldehyde in PBS, washed in 0.1% PBS Tween20 (Sigma-Aldrich) and permeabilized with 0.5% Triton-X100 (Sigma-Aldrich) in PBS for 20 min. Several washing steps were followed by 2 h blocking with 5% goat serum, 5% BSA, 20 mM MgCl2 in PBS followed by overnight incubation with the primary antibody at 4ºC. Secondary antibodies were diluted 1:500 in PBS and incubated for 3 h. Nuclei were counterstained with DAPI (Invitrogen) for 30 min. After several washes, embryos were mounted in Vectashield (Vector).

The antibodies for immunofluorescence detection were as follows: anti-myosin heavy chain (MF20, 2147781 DSHB) at a 1:20 dilution, anti-GFP (1010 Aveslab) at 1:1000, anti-β-catenin (610153, BD Transduction Laboratories) at 1:200 and anti-pH3 (06-570, Merck) at 1:100. Secondary antibodies were the following: anti-mouse IgG2b 568 (Invitrogen) and anti-chicken 488 (Life Technologies).

Embryos were imaged with a Zeiss 780 confocal microscope fitted with a 20× objective 1.0 NA with a water immersion lens. Z-stack images of the whole pericardial cavity were taken every 5 µm. Maximum projections of Z-stack images were 3D reconstructed in whole-mount views using Imaris software (Bitplane Scientific Software). The ventral pericardial layer was digitally removed to provide a clearer view of the heart tube and DP. Optical sections of 1 z-slice were also shown in some figures.

Definition of the dorsal pericardial tissue and proepicardium

PE clusters have been described to emerge from the DP layer, appearing from a region close to the avc in the vp of the heart tube surrounding area (Peralta et al., 2013). Because there is no specific marker that allows differentiating PE from pericardial cells, position and shape has been used to define PE. The dorsal pericardial tissue has a flat morphology and was labeled as the actual DP, while groups of cells with a rounded morphology on the DP close to the avc region were referred as the PE (Peralta et al., 2013; Andres-Delgado et al., 2019).

To estimate the roundness index (R index) of DP and avcPE, the height (h) and width (w) of those tissues were measured on *epi:GFP* 60 hpf zebrafish. In pericardial cavity images (2D optical sections from an images-stack), the h and the w of the right DP area and of the avcPE was measured using Image J software. A minimum of 4 images per animal were

measured. The ratio h / w gives the R index. The closer the R index is to 1, closer to the circumference will be the shape of the structure.

Digital isolation of the dorsal pericardium

In *epi:GFP* embryos, all EPDCs express GFP (Peralta et al., 2014). To favor the visualization of DP tissue in the 3D reconstructions of pericardial cavities, the ventral pericardium was removed from all images of the stack. Imaris software (Bitplane Scientific Software) Surface-Function was used to create a mask of the heart without the ventral pericardium, and 3D reconstruction of the heart cavity with the DP digitally isolated was done.

Volume estimation

Calculation of structures volume was performed using stereological Cavalieri's estimator (Gundersen et al., 1988; Cruz-Orive, 1999) from Image J: Volumest PlugIn Merzin, Markko ("Applying stereological method in radiology. Volume measurement. "Bachelor's thesis. University of Tartu. 2008). Images from a stack which comprises all the slices were the region of interest (DP or avcPE) appears were used**.**

The volume was estimated by the formula:

$$\boldsymbol{V} = \boldsymbol{t} \times \sum_{\mathbf{1}}^{\boldsymbol{n}} \boldsymbol{A}$$

t = actual thickness of slice. t = 5 μm.

n = number of slices where the region of interest appears.

A = area of interest were calculated using the Cavalieri´s estimator and were expressed in μm^2.

Intensity quantification

Anti-GFP-488 immunofluorescence intensity quantification (*epi:GFP* line) was calculated for DP and PE regions. A minimum of 8 slices from an images-stack were quantified, per animal, using Image J: Integrated Optical Density. The product of Area by Mean Gray Value (average gray value within the selected region) determined the GFP-Wt1a intensity level in the DP tissue or avcPE areas per animal.

In situ hybridization

In situ hybridization on whole-mount 60 hpf zebrafish embryos was performed as described (Jowett and Lettice, 1994), using riboprobes against full coding sequence of *wt1a* and *GFP* cDNAs (Peralta et al., 2013). Larvae were fixed in 4% PFA overnight, dehydrated in methanol series and stored at -20°C until use. On day 1, embryos were bleached in 1,5% of H_2O_2 in methanol, rehydrated, and digested with proteinase-K 10 $\mu g.ml^{-1}$ for 17 min. Endogenous alkaline phosphatase was blocked with triethanolamine 0,1 M, pH 8 with 0.25% of acetic anhydride for 20 min and re-fixed in 4% PFA for 20 min. After washing, they were pre-hybridized at 68°C for at least 1 h. The antisense riboprobe was added at 0.5 $\mu g.ml^{-1}$. After hybridization, several washes were done before overnight incubation with 1:4000 dilution of anti digoxigenin-AP antibody (Roche, 11093274910) in blocking solution (Roche, 11096176001). Embryos were developed in BM-Purple until signal was detected.

Statistical analysis

Student's t test for comparisons between two groups was used. The level of significance selected was $P < 0.05$. Calculations were made with Microsoft Excel and GraphPad. P-values are indicated either in the figure legends, the main text or summarized.

Results

Measurement of dorsal pericardium and proepicardium volume

At 60 hpf, the main PE cluster in zebrafish, the avcPE, appears on the DP tissue near the atrio-ventricular area (Fig. 1a). Z-stack images were taken every 5 µm, and 3D maximum projection reconstruction of the pericardial cavity was shown (Fig. 1a-1). 3D heart was rotated 45º on X-axis (Fig. 1a-2) to allow a better view of the PE at the avc site. Ventral pericardium was digitally removed (Fig. 1a-3).

The roundness of the pericardial tissues was determined using the Roundness Index (R). R is 0.028 ± 0.02 for DP tissue, whereas for PE is 12.5-fold more: 0.35 ± 0.083. PE tissue is more globular shaped than the flat DP tissue (Fig. 1b,c).

Continuing with the characterization of the PE tissue, we determined that despite the roundness of PE, the DP layer volume was significantly larger (133000 ± 67000 μm^3) than in the avcPE cluster (10700 ± 2070 μm^3, n = 6 animals) (Fig. 2a,b).

Proepicardial tissue presents increased GFP intensity level

Intensity level of GFP, as a reflection of the Wt1a level, using the *epi:GFP* zebrafish line, was measured both in DP and in PE tissue. Our results determined that PE GFP intensity per volume was significantly higher than in the DP layer of the same animal (n = 6 animals) (Fig.3).

Bmp2b overexpression increases proepicardium volume

In control *epi:GFP* animals subjected to heat shock (HS), the PE was normally formed and visible at 60 hpf. Overexpression of *bmp2b* using the transgenic line *Tg(hsp70l:bmp2b)* crossed into *epi:GFP*, resulted in a 2-fold enlargement in the PE tissue volume at 60 hpf (Fig. 4a). PE tissue volume in control was 10700 ± 2070 μm^3 compared with a volume of 23000 ± 2450 μm^3 upon *bmp2b* overexpression (n= 6 animals; P-value < 0.0001) (Fig. 4b). However, *bmp2b* overexpression does not affect the DP tissue layer volume.

We next aimed to assess whether the enhancement in the PE volume is due to PE cell proliferation favored by Bmp2b. To do this, we evaluated the expression of phospho-histone 3 (pH3), a biomarker that labels cells in mitosis. We detected that *bmp2b* overexpression does not affect the number of proliferating cells, neither in the DP (Fig. 5a,b) nor in the PE (Fig. 5a,c).

bmp2b overexpression increases GFP intensity level in the pericardium

We next wanted to investigate whether the Bmp pathway signaling can affect the intensity level of GFP, as a reflection of the Wt1a level, in the pericardial tissues. Using 60 hpf *epi:GFP* animals overexpressing *bmp2b*, GFP intensity per volume was higher in the PE cluster than in the DP tissue of the same *bmp2b*-overexpressed animal (n = 6 animals) (Fig. 6a,b).

We explored whether the enlargement of avcPE cluster volume observed upon *bmp2b* overexpression occurs concomitantly with an increase in GFP level. GFP intensity, was significantly different in DP compared to PE, both in control and upon *bmp2b* overexpression (Fig. 7a,b). Besides, we showed that Bmp2b can increase the GFP intensity level in the PE tissue (18.1 ± 4.01 Arbitrary Units (AU) in control versus 47.8 ± 14.7 AU in the PE of *bmp2b* overexpressing embryos, P-value = 0.0007)) (Fig. 7b). Interestingly, Bmp2b was also able to enhance GFP intensity level in the DP tissue (1.96 ± 0.796 AU in control versus 10.3 ± 5.3 AU in *bmp2b*-overexpressed DP, P-value = 0.0025) (Fig. 7b).

Finally, we compared the GFP intensity level per tissue volume. In PE, this value was much higher than in their DP layer (Fig. 7a,c). In the DP tissue, this signal was higher upon

bmp2b overexpression: 0.023 ± 0.008 AU/μm^3 in control compared to 0.075 ± 0.029 AU/μm^3 in *bmp2b* overexpress DP, P-value= 0.0021 (Fig. 7c). Regarding the PE, GFP level also was higher in animals overexpressing *bmp2b* (Fig. 7b), but taking into account that the volume of PE cluster is double sized by Bmp2b, significance here was not reported (0.647 ± 0.358 AU/μm^3 in control animals versus 0.968 ± 0.362 AU/μm^3 in the PE of embryos overexpressing *bmp2b*) (Fig. 7c).

bmp2b overexpression favors wt1a expression level in the pericardium

To confirm the observations in the *epi:GFP* transgenic line, we performed whole-mount *in situ* hybridization against *GFP* and the native *wt1a,* both in control and upon *bmp2b* overexpression (Fig. 8a). *GFP* and *wt1a* mRNA were detected at 60 hpf in zebrafish PE cluster and to a lesser extent in the DP tissue (Fig. 8b,c). Bmp2b increased the expression of *GFP* in both the PE and in the DP (Fig. 8b). *wt1a* expression is also affected by Bmp2b (Fig. 8c).

Discussion

Here, we show that *bmp2b* overexpression enhances *wt1a* level in the pericardial tissues, and Wt1a could be involved in the PE volume increasing observed in animals overexpressing *bmp2b*.

To our knowledge, there is no specific marker for PE cells or other pericardial-derived tissues. Epicardium, DP and PE are all positive for the same pericardial lineage markers (Zeng et al., 2011; Peralta et al., 2014; Meilhac et al., 2015). The lack of markers makes difficult the differentiation of PE from DP cells, the position and rounder shape of the PE clusters was used to discriminate them from DP cells (Peralta et al., 2013; Plavicki et al., 2014; Andres-Delgado et al., 2019). In zebrafish epicardial cells are heterogeneous based on the expression of candidate genes (Cao et al., 2016; Weinberger et al., 2020), but specific markers are required for further studies in the field. *Wt1* expression in the PE has also been described as crucial for its development (Moore et al., 1999; Pombal et al., 2008; Serluca, 2008; Zeng et al., 2011), and in zebrafish *wt1* transcription factor is expressed in PE and epicardium, and is necessary for the PE formation (Serluca, 2008). Using zebrafish *epi:GFP* line that recapitulates *wt1a* expression (Peralta et al., 2013), we show that the GFP intensity signal and the *wt1a* expression level are significantly higher in avcPE cluster compared to DP tissue, which can be used to differentiate PE cells from DP tissue and will help to describe new PE characteristics. In mice, WT1 presence in the PE organ is mediated by NX2.5 (Zhou et al., 2008), and in chicks, proepicardial markers such as Tbx18 or Wt1 upregulation are mediated by FGF8 and Snail1 via the Twist1 molecule (Schlueter and Brand, 2009; Braitsch and Yutzey, 2013). Forced

expression of TWIST1 leads to PE formation (Schlueter and Brand, 2013) while absence of Tbx18 in embryos also exhibits proepicardial abnormalities (Kao et al., 2015). Wt1 has important functions during PE formation across species, and its expression level in the pericardial tissues might influence PE emergence.

Changes in the tissue specification mechanisms have to take place in the DP cells to allow its differentiation into PE (Andres-Delgado et al., 2019). Our results could indicate that higher expression of Wt1 in the PE benefits its EMT-like process of roundness from the flat DP layer. WT1 is key in the morphogenesis of different structures (Chau and Hastie, 2012), and has been implicated in the specification of EMT phenotype (Huang et al., 2012; Artibani et al., 2017). During development of certain mesodermal tissues, *Wt1* regulates mesenchymal cell maintenance, and depending on the context, loss of *Wt1* can induce mesenchymal to epithelial cell shift or the reverse process (Ocana et al., 2012; Rivas et al., 2013). In epicardium, WT1 acts in maintaining an intact epithelial cell morphology (Martinez-Estrada et al., 2010; Bax et al., 2011), while WT1 null mice are not viable (Kreidberg et al., 1993; Moore et al., 1999; Carmona et al., 2001). In human epicardial cells, *WT1* knockdown stimulates the loss of epithelial morphology, the reduction of the expression of *E-cadherin*, *α4-integrin* and *VCAM-1* and the significantly increase of *Snai1* (Bax et al., 2011), but the opposite results were also described (Martinez-Estrada et al., 2010; von Gise et al., 2011). Together, all these findings suggest that WT1 plays a major role regulating the balance between epithelial-mesenquimal phenotypes, two fundamental cell states in mesodermal tissues.

Apical extrusion is a cellular mechanism that controls epithelial layer homeostasis, and it takes place in the intestine while preserving its barrier function (Norden et al., 2009; Simovitch et al., 2010; Ritchie et al., 2012) or during embryogenesis to control cell number. Thereby, supernumerary cells have to be eliminated towards the apical side, with the consequent death of extruded cells due to loss of survival factors (Eisenhoffer et al., 2012; Marinari et al., 2012). On the contrary, in cancer, transformed cells can live and extrude. WT1 overexpression has also been implicated in cancer progression due to its anti-apoptotic effect (Hartkamp et al., 2010). In PE formation process, the increased Wt1 level might be maintaining the PE cell in an alive state until attachment to myocardium.

Bmp pathway has been found to be involved in PE formation process in mice (del Monte et al., 2011) and chicken (Schlueter et al., 2006) where after Bmp2 addition *Wt1* is downregulated in PE. In zebrafish, mutants for the Bmp receptor acvr1l or animals inhibited with a Bmp antagonist do not form a PE, whereas *bmp2b* overexpression extends PE (Liu and Stainier, 2010; Andres-Delgado et al., 2019). Here, we show than in zebrafish Bmp2b increased *wt1a* in the PE and interestingly, in the DP tissue as well. *bmp2b* overexpression also correlates with a bigger PE, suggesting that increased Wt1 level in DP and PE affects positively to the PE formation process in zebrafish.

In conclusion, we propose a model in which Bmp pathway signaling promotes Wt1 level in the DP tissue, which enhances the process of PE extrusion. Maintenance of high level of Wt1 in the PE cells might favors cells mesenchymal state and apoptosis inhibition until attachment to myocardium.

Acknowledgements

We are grateful to the Animal Facility and Microscopy Unit at Nacional Center of Cardiovascular Research Carlos III.

References

Andres-Delgado L. and Mercader N. (2016). Interplay between cardiac function and heart development. Biochim. Biophys. Acta. 1863, 1707-1716.

Andres-Delgado L., Ernst A., Galardi-Castilla M., Bazaga D., Peralta M., Munch J., Gonzalez-Rosa J.M., Marques I., Tessadori F., de la Pompa J.L., Vermot J. and Mercader N. (2019). Actin dynamics and the bmp pathway drive apical extrusion of proepicardial cells. Development. 146.

Artibani M., Sims A.H., Slight J., Aitken S., Thornburn A., Muir M., Brunton V.G., Del-Pozo J., Morrison L.R., Katz E., Hastie N.D. and Hohenstein P. (2017). Wt1 expression in breast cancer disrupts the epithelial/mesenchymal balance of tumour cells and correlates with the metabolic response to docetaxel. Sci. Rep. 7, 45255.

Bax N.A., van Oorschot A.A., Maas S., Braun J., van Tuyn J., de Vries A.A., Groot A.C. and Goumans M.J. (2011). In vitro epithelial-to-mesenchymal transformation in human adult epicardial cells is regulated by tgfbeta-signaling and wt1. Basic. Res. Cardiol. 106, 829-847.

Braitsch C.M. and Yutzey K.E. (2013). Transcriptional control of cell lineage development in epicardium-derived cells. J. Dev. Biol. 1, 92-111.

Cao J., Navis A., Cox B.D., Dickson A.L., Gemberling M., Karra R., Bagnat M. and Poss K.D. (2016). Single epicardial cell transcriptome sequencing identifies caveolin 1 as an essential factor in zebrafish heart regeneration. Development. 143, 232-243.

Carmona R., Gonzalez-Iriarte M., Perez-Pomares J.M. and Munoz-Chapuli R. (2001). Localization of the wilm's tumour protein wt1 in avian embryos. Cell. Tissue. Res. 303, 173-186.

Collins M.M. and Stainier D.Y. (2016). Organ function as a modulator of organ formation: Lessons from zebrafish. Curr. Top. Dev. Biol. 117, 417-433.

Cruz-Orive L.M. (1999). Unbiased stereology: Three-dimensional measurement in microscopy. J. Anat. 194, 153-157.

Chau Y.Y. and Hastie N.D. (2012). The role of wt1 in regulating mesenchyme in cancer, development, and tissue homeostasis. Trends. Genet. 28, 515-524.

Chau Y.Y., Bandiera R., Serrels A., Martinez-Estrada O.M., Qing W., Lee M., Slight J., Thornburn A., Berry R., McHaffie S., Stimson R.H., Walker B.R., Chapuli R.M., Schedl A. and Hastie N. (2014). Visceral and subcutaneous fat have different origins and evidence supports a mesothelial source. Nat. Cell. Biol. 16, 367-375.

Chocron S., Verhoeven M.C., Rentzsch F., Hammerschmidt M. and Bakkers J. (2007). Zebrafish bmp4 regulates left-right asymmetry at two distinct developmental time points. Dev. Biol. 305, 577-588.

del Monte G., Casanova J.C., Guadix J.A., MacGrogan D., Burch J.B., Perez-Pomares J.M. and de la Pompa J.L. (2011). Differential notch signaling in the epicardium is required for cardiac inflow development and coronary vessel morphogenesis. Circ. Res. 108, 824-836.

Duenas A., Aranega A.E. and Franco D. (2017). More than just a simple cardiac envelope; cellular contributions of the epicardium. Front. Cell. Dev. Biol. 5, 44.

Eisenhoffer G.T., Loftus P.D., Yoshigi M., Otsuna H., Chien C.B., Morcos P.A. and Rosenblatt J. (2012). Crowding induces live cell extrusion to maintain homeostatic cell numbers in epithelia. Nature. 484, 546-549.

Gundersen H.J., Bagger P., Bendtsen T.F., Evans S.M., Korbo L., Marcussen N., Moller A., Nielsen K., Nyengaard J.R., Pakkenberg B. and et al. (1988). The new stereological tools: Disector, fractionator, nucleator and point sampled intercepts and their use in pathological research and diagnosis. APMIS. 96, 857-881.

Hartkamp J., Carpenter B. and Roberts S.G. (2010). The wilms' tumor suppressor protein wt1 is processed by the serine protease htra2/omi. Mol. Cell. 37, 159-171.

Huang B., Pi L., Chen C., Yuan F., Zhou Q., Teng J. and Jiang T. (2012). Wt1 and pax2 re-expression is required for epithelial-mesenchymal transition in 5/6 nephrectomized rats and cultured kidney tubular epithelial cells. Cells. Tissues. Organs. 195, 296-312.

Jowett T. and Lettice L. (1994). Whole-mount in situ hybridizations on zebrafish embryos using a mixture of digoxigenin- and fluorescein-labelled probes. Trends. Genet. 10, 73-74.

Kao R.M., Rurik J.G., Farr G.H., 3rd, Dong X.R., Majesky M.W. and Maves L. (2015). Pbx4 is required for the temporal onset of zebrafish myocardial differentiation. J. Dev. Biol. 3, 93-111.

Kennedy-Lydon T. and Rosenthal N. (2015). Cardiac regeneration: Epicardial mediated repair. Proc. Biol. Sci. 282, 20152147.

Kreidberg J.A., Sariola H., Loring J.M., Maeda M., Pelletier J., Housman D. and Jaenisch R. (1993). Wt-1 is required for early kidney development. Cell. 74, 679-691.

Li J., Miao L., Zhao C., Shaikh Qureshi W.M., Shieh D., Guo H., Lu Y., Hu S., Huang A., Zhang L., Cai C.L., Wan L.Q., Xin H., Vincent P., Singer H.A., Zheng Y., Cleaver O., Fan Z.C. and Wu M. (2017). Cdc42 is required for epicardial and pro-epicardial development by mediating fgf receptor trafficking to the plasma membrane. Development. 144, 1635-1647.

Liu J. and Stainier D.Y. (2010). Tbx5 and bmp signaling are essential for proepicardium specification in zebrafish. Circ. Res. 106, 1818-1828.

Manner J., Perez-Pomares J.M., Macias D. and Munoz-Chapuli R. (2001). The origin, formation and developmental significance of the epicardium: A review. Cells. Tissues. Organs. 169, 89-103.

Marinari E., Mehonic A., Curran S., Gale J., Duke T. and Baum B. (2012). Live-cell delamination counterbalances epithelial growth to limit tissue overcrowding. Nature. 484, 542-545.

Martinez-Estrada O.M., Lettice L.A., Essafi A., Guadix J.A., Slight J., Velecela V., Hall E., Reichmann J., Devenney P.S., Hohenstein P., Hosen N., Hill R.E., Munoz-Chapuli R. and Hastie N.D. (2010). Wt1 is required for cardiovascular progenitor cell formation through transcriptional control of snail and e-cadherin. Nat. Genet. 42, 89-93.

Maya-Ramos L., Cleland J., Bressan M. and Mikawa T. (2013). Induction of the proepicardium. J. Dev. Biol. 1, 82-91.

Meilhac S.M., Lescroart F., Blanpain C. and Buckingham M.E. (2015). Cardiac cell lineages that form the heart. Cold Spring Harb. Perspect. Med. 5, a026344.

Moore A.W., McInnes L., Kreidberg J., Hastie N.D. and Schedl A. (1999). Yac complementation shows a requirement for wt1 in the development of epicardium, adrenal gland and throughout nephrogenesis. Development. 126, 1845-1857.

Nahirney P.C., Mikawa T. and Fischman D.A. (2003). Evidence for an extracellular matrix bridge guiding proepicardial cell migration to the myocardium of chick embryos. Dev. Dyn. 227, 511-523.

Norden C., Young S., Link B.A. and Harris W.A. (2009). Actomyosin is the main driver of interkinetic nuclear migration in the retina. Cell. 138, 1195-1208.

Ocana O.H., Coskun H., Minguillon C., Murawala P., Tanaka E.M., Galceran J., Munoz-Chapuli R. and Nieto M.A. (2017). A right-handed signalling pathway drives heart looping in vertebrates. Nature. 549, 86-90.

Ocana O.H., Corcoles R., Fabra A., Moreno-Bueno G., Acloque H., Vega S., Barrallo-Gimeno A., Cano A. and Nieto M.A. (2012). Metastatic colonization requires the repression of the epithelial-mesenchymal transition inducer prrx1. Cancer. Cell. 22, 709-724.

Olivey H.E. and Svensson E.C. (2010). Epicardial-myocardial signaling directing coronary vasculogenesis. Circ. Res. 106, 818-832.

Peralta M., Gonzalez-Rosa J.M., Marques I.J. and Mercader N. (2014). The epicardium in the embryonic and adult zebrafish. J. Dev. Biol. 2, 101-116.

Peralta M., Steed E., Harlepp S., Gonzalez-Rosa J.M., Monduc F., Ariza-Cosano A., Cortes A., Rayon T., Gomez-Skarmeta J.L., Zapata A., Vermot J. and Mercader N. (2013). Heartbeat-driven pericardiac fluid forces contribute to epicardium morphogenesis. Curr. Biol. 23, 1726-1735.

Perez-Pomares J.M. and de la Pompa J.L. (2011). Signaling during epicardium and coronary vessel development. Circ. Res. 109, 1429-1442.

Perez-Pomares J.M., Phelps A., Sedmerova M. and Wessels A. (2003). Epicardial-like cells on the distal arterial end of the cardiac outflow tract do not derive from the proepicardium but are derivatives of the cephalic pericardium. Dev. Dyn. 227, 56-68.

Plavicki J.S., Hofsteen P., Yue M.S., Lanham K.A., Peterson R.E. and Heideman W. (2014). Multiple modes of proepicardial cell migration require heartbeat. BMC. Dev. Biol. 14, 18.

Pombal M.A., Carmona R., Megias M., Ruiz A., Perez-Pomares J.M. and Munoz-Chapuli R. (2008). Epicardial development in lamprey supports an evolutionary origin of the vertebrate epicardium from an ancestral pronephric external glomerulus. Evol. Dev. 10, 210-216.

Ritchie J.M., Rui H., Zhou X., Iida T., Kodoma T., Ito S., Davis B.M., Bronson R.T. and Waldor M.K. (2012). Inflammation and disintegration of intestinal villi in an experimental model for vibrio parahaemolyticus-induced diarrhea. PLoS. Pathog. 8, e1002593.

Rivas V., Carmona R., Munoz-Chapuli R., Mendiola M., Nogues L., Reglero C., Miguel-Martin M., Garcia-Escudero R., Dorn G.W., 2nd, Hardisson D., Mayor F., Jr. and Penela P. (2013). Developmental and tumoral vascularization is regulated by g protein-coupled receptor kinase 2. J. Clin. Invest. 123, 4714-4730.

Rodgers L.S., Lalani S., Runyan R.B. and Camenisch T.D. (2008). Differential growth and multicellular villi direct proepicardial translocation to the developing mouse heart. Dev. Dyn. 237, 145-152.

Schlueter J. and Brand T. (2009). A right-sided pathway involving fgf8/snai1 controls asymmetric development of the proepicardium in the chick embryo. Proc. Natl. Acad. Sci. 106, 7485-7490.

Schlueter J. and Brand T. (2013). Subpopulation of proepicardial cells is derived from the somatic mesoderm in the chick embryo. Circ. Res. 113, 1128-1137.

Schlueter J., Manner J. and Brand T. (2006). Bmp is an important regulator of proepicardial identity in the chick embryo. Dev. Biol. 295, 546-558.

Schulte I., Schlueter J., Abu-Issa R., Brand T. and Manner J. (2007). Morphological and molecular left-right asymmetries in the development of the proepicardium: A comparative analysis on mouse and chick embryos. Dev. Dyn. 236, 684-695.

Serluca F.C. (2008). Development of the proepicardial organ in the zebrafish. Dev. Biol. 315, 18-27.

Simoes F.C. and Riley P.R. (2018). The ontogeny, activation and function of the epicardium during heart development and regeneration. Development. 145.

Simovitch M., Sason H., Cohen S., Zahavi E.E., Melamed-Book N., Weiss A., Aroeti B. and Rosenshine I. (2010). Espm inhibits pedestal formation by enterohaemorrhagic escherichia coli and enteropathogenic e. Coli and disrupts the architecture of a polarized epithelial monolayer. Cell. Microbiol. 12, 489-505.

Smart N., Bollini S., Dube K.N., Vieira J.M., Zhou B., Davidson S., Yellon D., Riegler J., Price A.N., Lythgoe M.F., Pu W.T. and Riley P.R. (2011). De novo cardiomyocytes from within the activated adult heart after injury. Nature. 474, 640-644.

Steed E., Boselli F. and Vermot J. (2016). Hemodynamics driven cardiac valve morphogenesis. Biochim. Biophys. Acta. 1863, 1760-1766.

Tandon P., Wilczewski C.M., Williams C.E. and Conlon F.L. (2016). The lhx9-integrin pathway is essential for positioning of the proepicardial organ. Development. 143, 831-840.

von Gise A., Zhou B., Honor L.B., Ma Q., Petryk A. and Pu W.T. (2011). Wt1 regulates epicardial epithelial to mesenchymal transition through beta-catenin and retinoic acid signaling pathways. Dev. Biol. 356, 421-431.

Weinberger M., Simoes F.C., Patient R., Sauka-Spengler T. and Riley P.R. (2020). Functional heterogeneity within the developing zebrafish epicardium. Dev. Cell. 52, 574-590.e576.

Wessels A., van den Hoff M.J., Adamo R.F., Phelps A.L., Lockhart M.M., Sauls K., Briggs L.E., Norris R.A., van Wijk B., Perez-Pomares J.M., Dettman R.W. and Burch J.B. (2012). Epicardially derived fibroblasts preferentially contribute to the parietal leaflets of the atrioventricular valves in the murine heart. Dev. Biol. 366, 111-124.

Wu M., Smith C.L., Hall J.A., Lee I., Luby-Phelps K. and Tallquist M.D. (2010). Epicardial spindle orientation controls cell entry into the myocardium. Dev. Cell. 19, 114-125.

Zeng B., Ren X.F., Cao F., Zhou X.Y. and Zhang J. (2011). Developmental patterns and characteristics of epicardial cell markers tbx18 and wt1 in murine embryonic heart. J. Biomed. Sci. 18, 67.

Zhou B., von Gise A., Ma Q., Rivera-Feliciano J. and Pu W.T. (2008). Nkx2-5- and isl1-expressing cardiac progenitors contribute to proepicardium. Biochem. Biophys. Res. Commun. 375, 450-453.

Figure Legends:

Fig. 1. Proepicardium is more rounded than the dorsal pericardial tissue. (a) 3D maximum projections of a 60 hpf zebrafish heart. *epi:GFP* embryos immunostained for GFP (green) and myosin heavy chain (MHC) (red). a1, Distance between slices is 5 μm; a2, 3D image a1 was rotated 45º in the X-axis; a3, in image a2 ventral pericardium had been digitally removed to provide a clearer view of the DP layer and the PE. Arrowheads, DP layer or avcPE cluster. **(b)** Top panel, optical section of a 60 hpf zebrafish heart, and zoomed images below. *epi:GFP* embryos immunostained for GFP (green), β-catenin (red) and nuclei were counterstained with DAPI (blue). Arrowheads, DP layer or avcPE cluster. White lines illustrate the height and width of DP layer or avcPE. **(c)** Quantification of DP and PE tissue roundness index (R) (n=6 animals). at, atrium; avc, atrio-ventricular canal; DP, dorsal pericardium; h, height; hpf, hours post fertilization; PE, proepicardium; R, roundness index; v, ventricle; w, width; Scale bar: 50 μm. Data are mean ± s.d., unpaired two-tailed Student's *t*-test. ***P < 0.001.

Fig. 2. Dorsal pericardial tissue volume is bigger than in proepicardium. **(a)** Top panel, optical section of a 60 hpf zebrafish heart, and zoomed images below. *epi:GFP* embryos immunostained for GFP (green), myosin heavy chain (MHC) (red) and nuclei were counterstained with DAPI (blue). Arrowheads, DP layer or avcPE cluster. White ellipses indicate the position of DP tissue or avcPE. **(b)** Quantification of DP and PE volume (n=6 animals). at, atrium; DP, dorsal pericardium; hpf, hours post fertilization; PE, proepicardium; v, ventricle; Scale bar: 50 μm. Data are mean ± s.d., unpaired two-tailed Student's *t*-test. ***P < 0.001.

Fig. 3. Proepicardium presents increased GFP intensity level compared to the dorsal pericardial tissue. Quantification of DP and PE GFP intensity signal per tissue volume in 6 60 hpf animals. AU, arbitrary units; DP, dorsal pericardium; PE, proepicardium; Data are mean ± s.d., unpaired two-tailed Student's *t*-test. ***P < 0.001.

Fig. 4. *bmp2b* overexpression increases proepicardium volume. (a) 3D maximum projections of 60 hpf zebrafish hearts. *epi:GFP* embryos immunostained for GFP (green) and myosin heavy chain (MHC) (red). Control compared with an animal overexpressing *bmp2b*. Arrowheads, DP layer or avcPE cluster. **(b)** Quantification of DP and PE volume from conditions shown in **a** (n=6 animals). at, atrium; DP, dorsal pericardium; hpf, hours post

fertilization; PE, proepicardium; v, ventricle; Scale bar: 50 μm. Data are mean ± s.d., unpaired two-tailed Student's *t*-test. ***$P < 0.001$, ns-non significant.

Fig. 5. (a) *bmp2b* overexpression does not affect pericardial cell proliferation. (**a**) *epi:GFP* embryos immunostained for GFP (green), myosin heavy chain (MHC) (red), pH3 (white) and nuclei counterstained with DAPI (blue). Top panels, 3D projection of 60 hpf zebrafish hearts, middle panels optical sections and zoomed images below. Control compared with an animal overexpressing *bmp2b*. Arrowheads, DP layer or avcPE cluster. Arrows, DP $pH3^+$ cells. Yellow arrowheads, PE cells, all negative for pH3. (**b, c**) Quantification of $pH3^+$ cells number in the DP (**b**) or in the PE (**c**) (n=6 animals). at, atrium; hpf; hours post fertilization; PE, proepicardium; v, ventricle. Scale bars: 50 μm (20 μm in zoomed **a**). Data are mean ± s.d.., unpaired two-tailed Student's *t*-test. ns-non significant.

Fig. 6. Upon *bmp2b* overexpression proepicardium presents increased GFP intensity level compared to the dorsal pericardial layer. (a) Top panel, optical section of a 60 hpf *bmp2b* overexpressing zebrafish heart, and zoomed images below. *epi:GFP* embryos immunostained for GFP (green), myosin heavy chain (MHC) (red) and nuclei were counterstained with DAPI (blue). Arrowheads, DP layer or avcPE cluster. White ellipses indicate the position of DP tissue or avcPE. **(b)** Quantification of DP and PE GFP intensity signal per tissue volume in 6 60 hpf animals. at, atrium; AU, arbitrary units; DP, dorsal pericardium; hpf, hours post fertilization; PE, proepicardium; v, ventricle; Scale bar: 50 μm. Data are mean ± s.d., unpaired two-tailed Student's *t*-test. ***$P < 0.001$.

Fig. 7. *bmp2b* overexpression increases GFP intensity level both in the proepicardium and in the dorsal pericardial tissue. (a) Top panel, optical sections of 60 hpf zebrafish hearts, and zoomed images below. *epi:GFP* embryos immunostained for GFP (green), myosin heavy chain (MHC) (red) and nuclei were counterstained with DAPI (blue). Control compared with an animal overexpressing *bmp2b*. Arrowheads, DP layer or avcPE cluster. **(b)** Quantification of DP and PE GFP intensity. **(c)** Quantification of DP and PE GFP intensity per tissue volume (n=6 animals). at, atrium; AU, arbitrary units; DP, dorsal pericardium; hpf, hours post fertilization; PE, proepicardium; v, ventricle; Scale bar: 50 μm. Data are mean ± s.d., unpaired two-tailed Student's *t*-test. **$P < 0.01$, ***$P < 0.001$, ns-non significant.

Fig. 8. *bmp2b* overexpression affects *wt1a* expression level in the pericardial tissues. (a) Whole-mount *in situ* hybridization for *GFP* and *wt1a* in control and *bmp2b* overexpressing animals at 60 hpf. White arrows, DP. Black arrows, avcPE. A representative animal is shown for each condition. Number of animal with the expression phenotype shown are indicated in the right corner. **(b)** Quantification of DP and PE *GFP in situ* hybridization intensity mean (n=8 animals in control and 7 *bmp2b* overexpressing animals). **(c)** Quantification of DP and PE *wt1a in situ* hybridization intensity mean (n=5 animals in control and 9 *bmp2b* overexpressing animals). AU, arbitrary units; DP, dorsal pericardium; hpf, hours post fertilization; PE, proepicardium; Scale bar: 50 µm. Data are mean ± s.d., unpaired two-tailed Student's *t*-test. **P* < 0.05, ***P* < 0.01, ns-non significant.

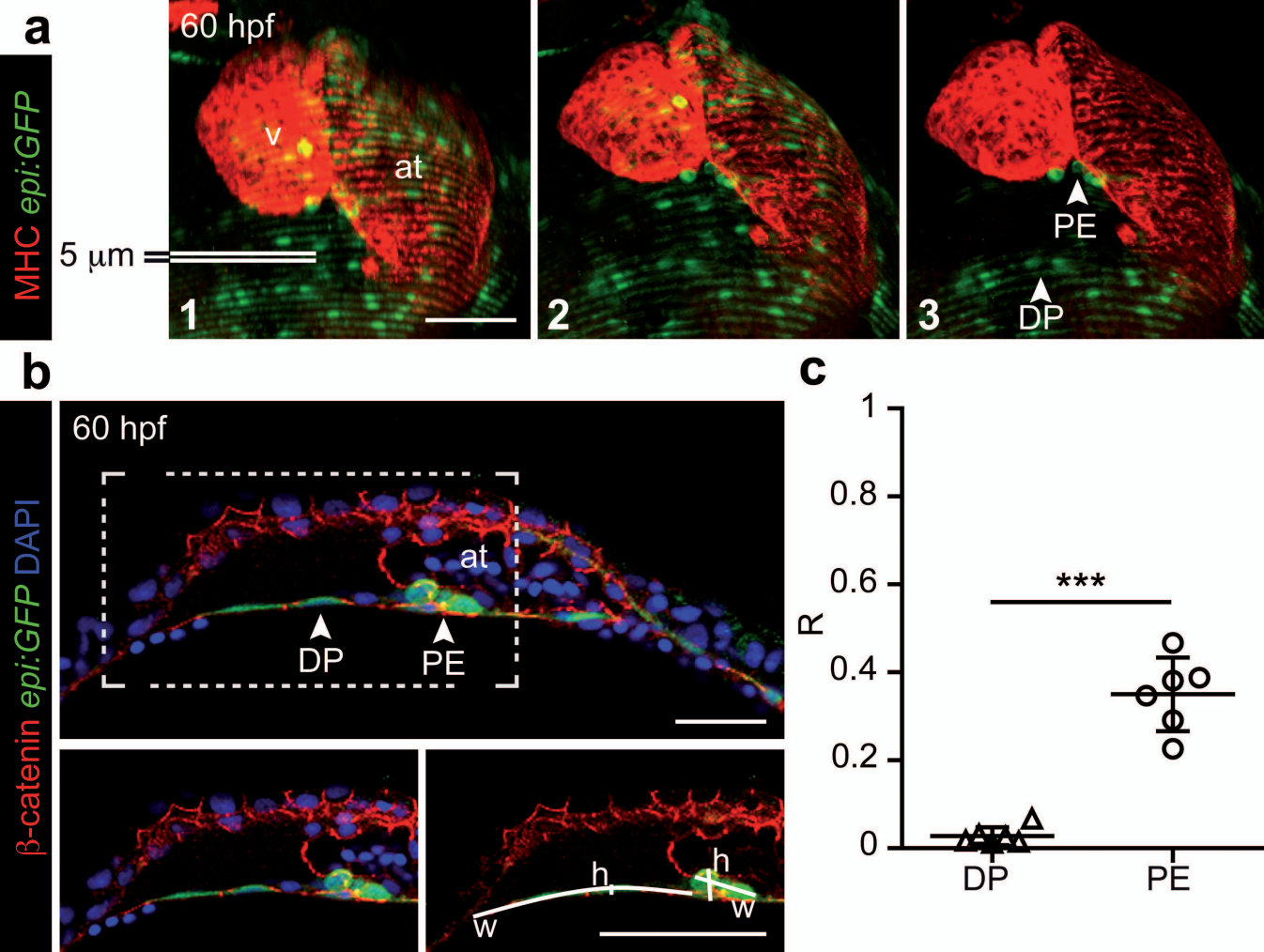
a
MHC epi:GFP
60 hpf
v
at
5 μm
1
2
3
PE
DP
b
β-catenin epi:GFP DAPI
60 hpf
at
DP
PE
h
w
c
R
1
0.8
0.6
0.4
0.2
0
***
DP
PE

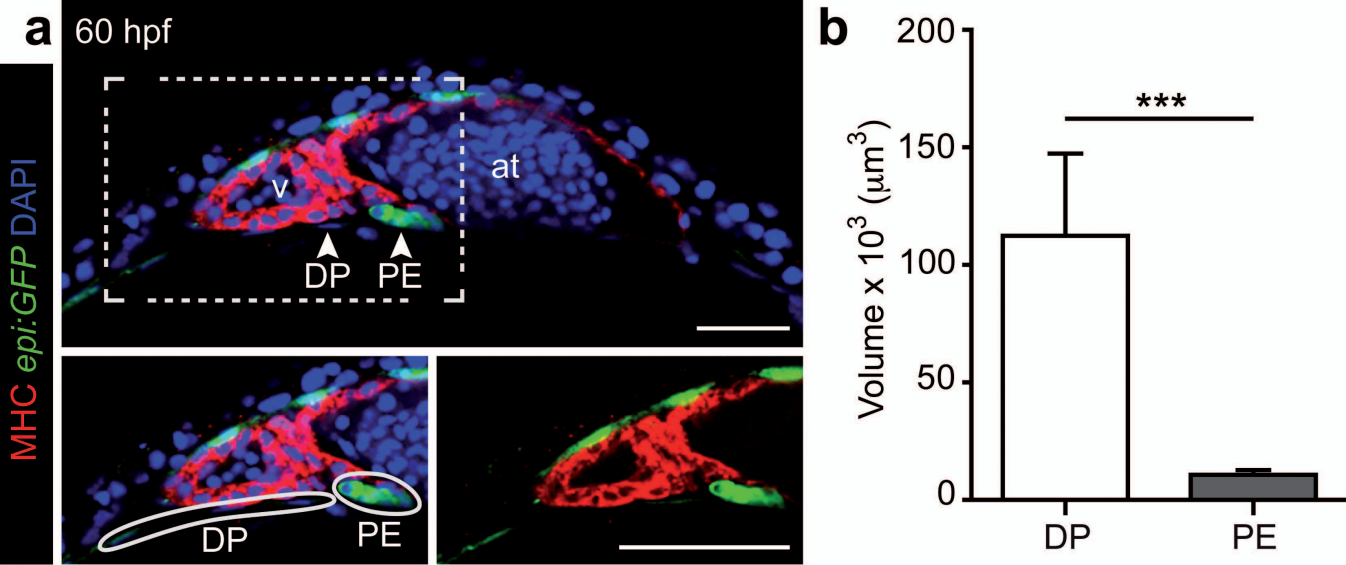
a
60 hpf
MHC epi:GFP DAPI
v
at
DP
PE
DP
PE
b
Volume x 10^3 (μm^3)
200
150
100
50
0
***
DP
PE

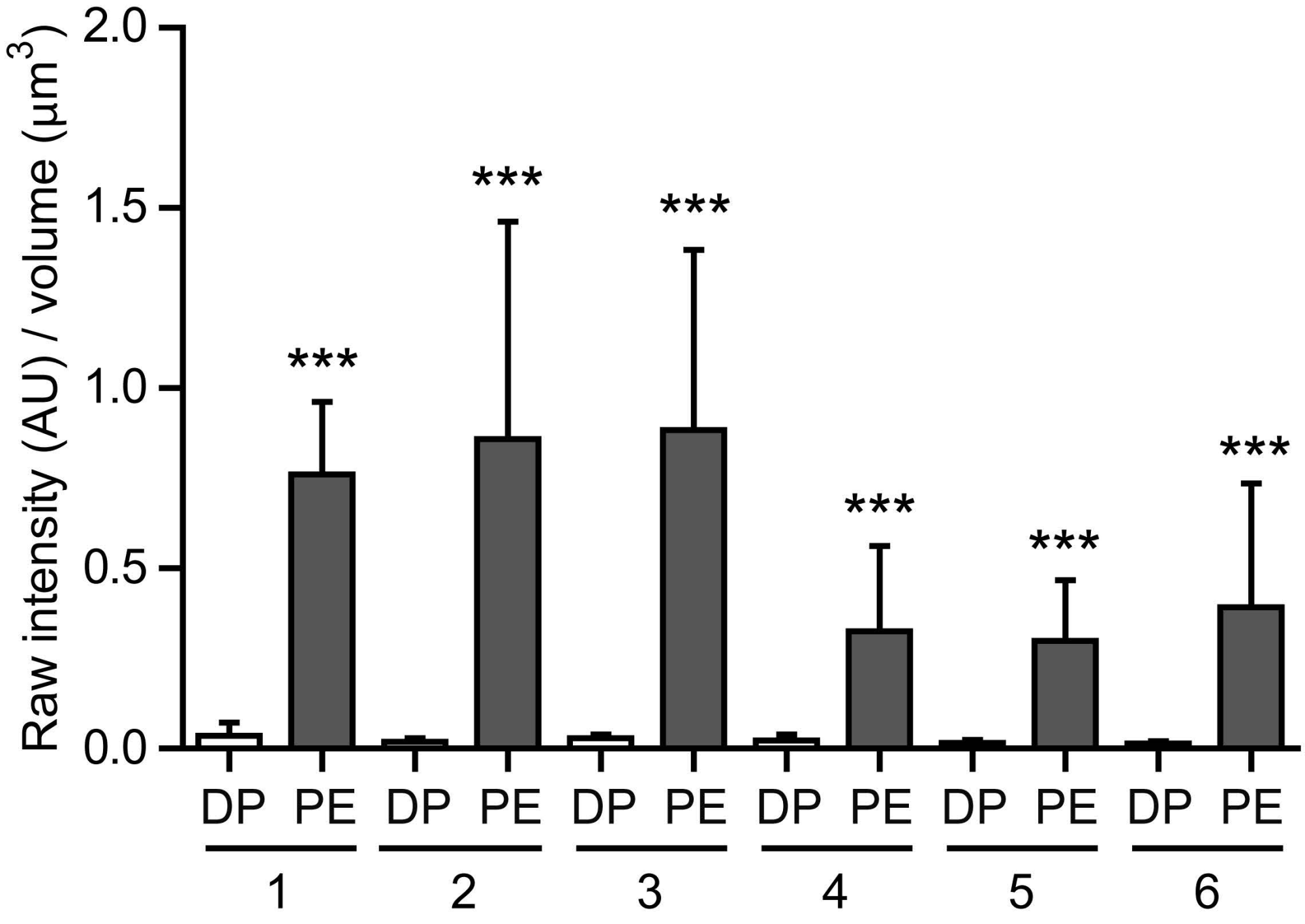
Raw intensity (AU) / volume (µm3)
2.0
1.5
1.0
0.5
0.0
***
***
***
***
***
***
DP PE DP PE DP PE DP PE DP PE DP PE
1
2
3
4
5
6

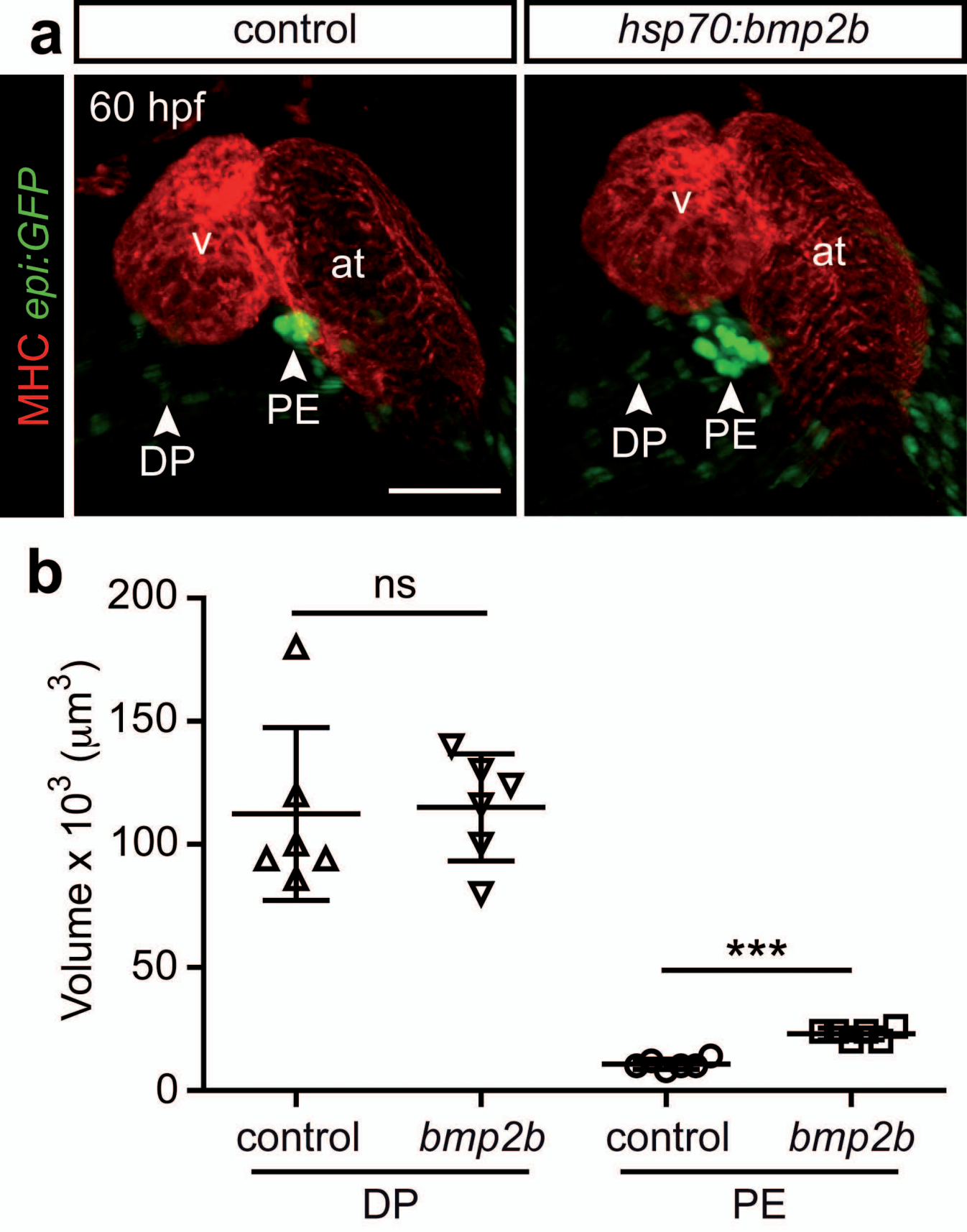
a
control
hsp70:bmp2b
MHC epi:GFP
60 hpf
v
at
PE
DP
v
at
DP
PE
b
200
150
100
50
0
Volume x 10^3 (μm^3)
ns
***
control
bmp2b
control
bmp2b
DP
PE

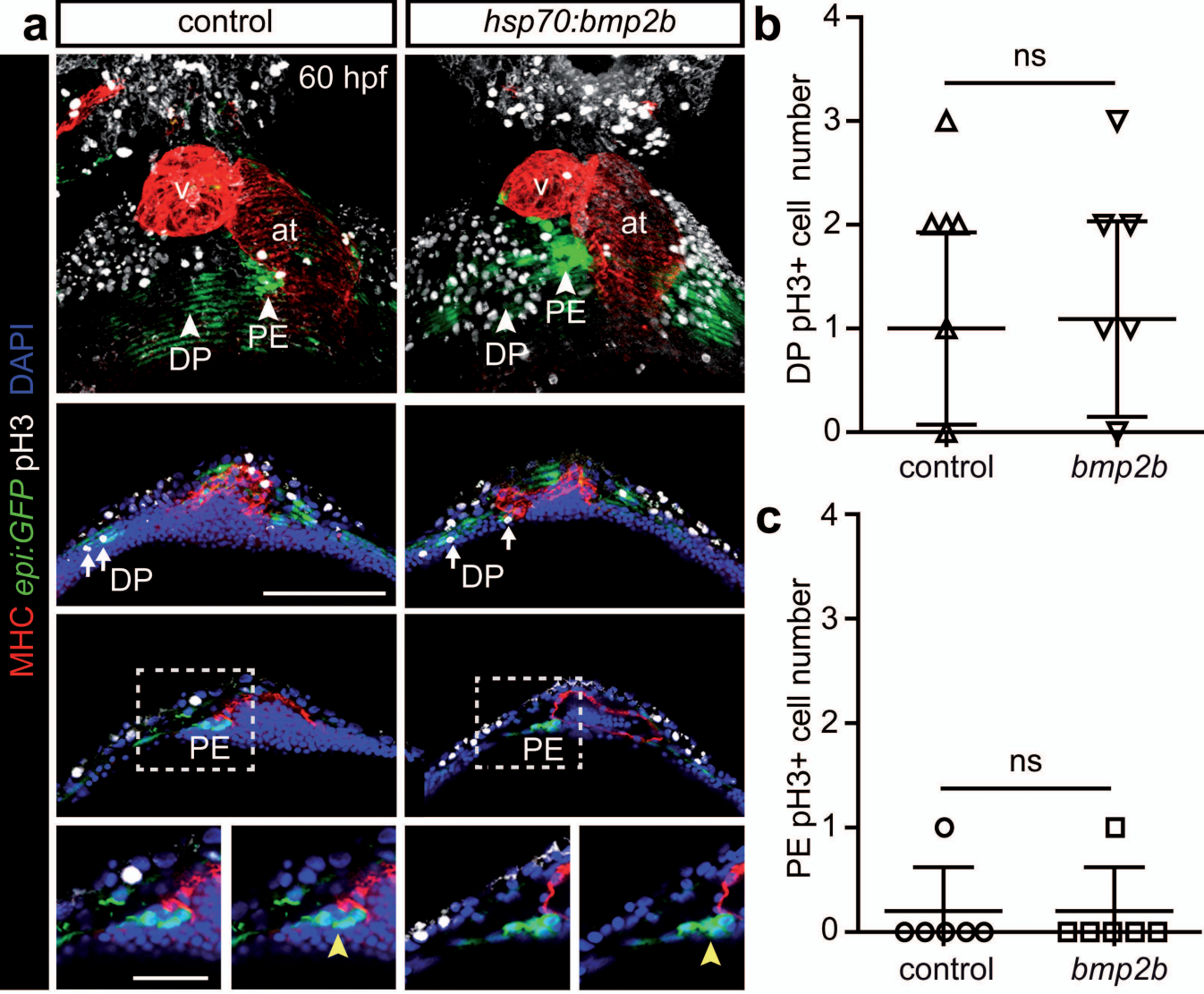
a
control
hsp70:bmp2b
60 hpf
v
at
DP
PE
MHC epi:GFP pH3 DAPI
b
DP pH3+ cell number
ns
control
bmp2b
c
PE pH3+ cell number
ns
control
bmp2b

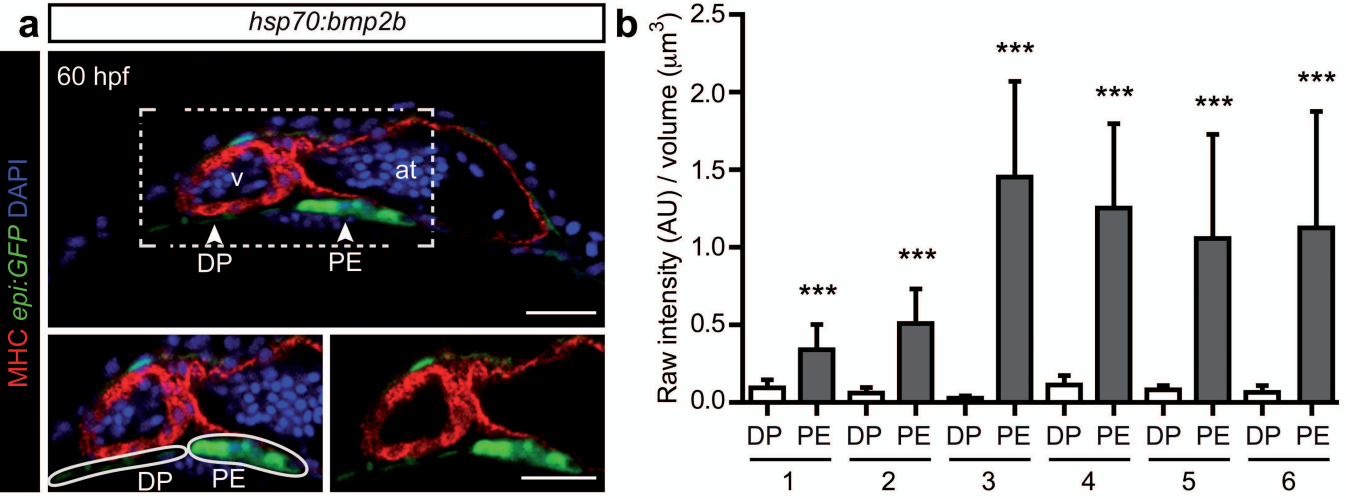
a
hsp70:bmp2b
60 hpf
v
at
DP
PE
MHC epi:GFP DAPI
DP
PE
b
Raw intensity (AU) / volume (μm3)
2.5
2.0
1.5
1.0
0.5
0.0
***
DP PE DP PE DP PE DP PE DP PE DP PE
1 2 3 4 5 6

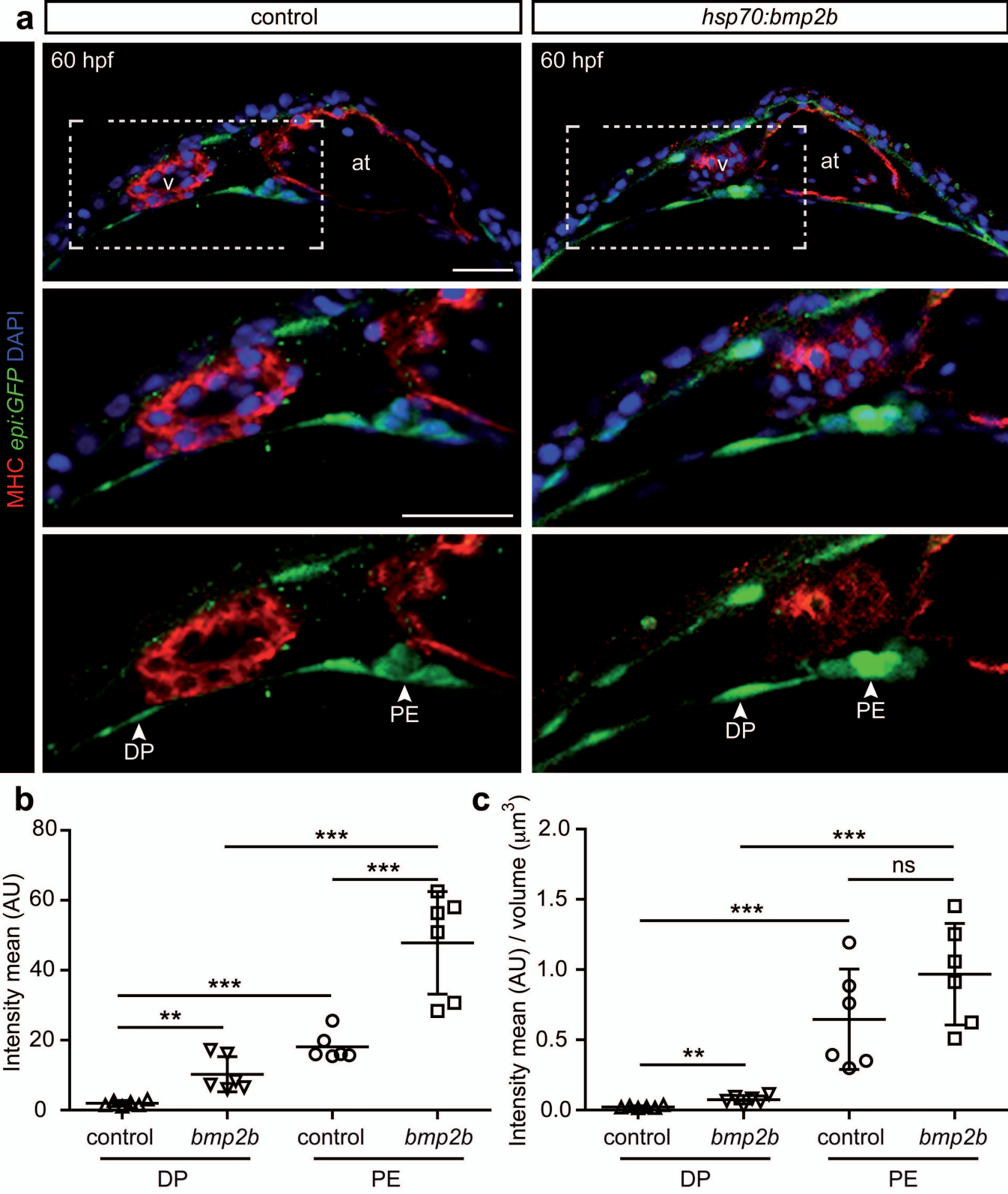
a
control
hsp70:bmp2b
60 hpf
60 hpf
v
at
v
at
MHC epi:GFP DAPI
DP
PE
DP
PE
b
Intensity mean (AU)
80
60
40
20
0
***
***
***
**
control
bmp2b
control
bmp2b
DP
PE
c
Intensity mean (AU) / volume (μm3)
2.0
1.5
1.0
0.5
0.0
***
ns
***
**
control
bmp2b
control
bmp2b
DP
PE

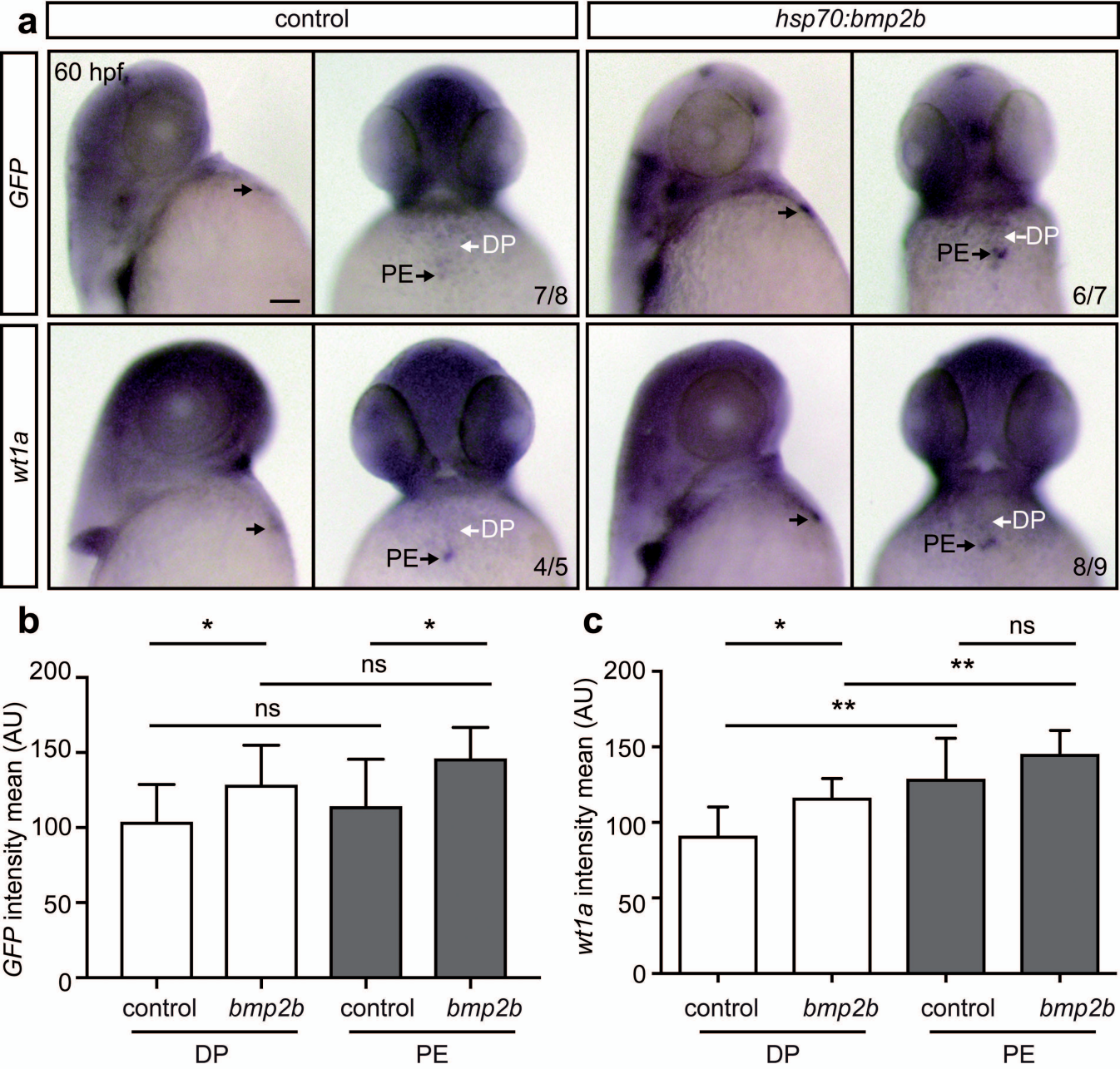
a
control
hsp70:bmp2b
GFP
wt1a
60 hpf
DP
PE
7/8
6/7
4/5
8/9
b
GFP intensity mean (AU)
200
150
100
50
0
*
*
ns
ns
control
bmp2b
control
bmp2b
DP
PE
c
wt1a intensity mean (AU)
200
150
100
50
0
*
ns
**
**
control
bmp2b
control
bmp2b
DP
PE

$$V = t \times \sum_{1}^{n} A$$